Feasibility analysis of a thermo-hydraulic process for reverse osmosis desalination : experimental approach

Clément Lacroix, B Guillaume, Maxime Perier-Muzet, Driss Stitou

Journal Pre-proofs

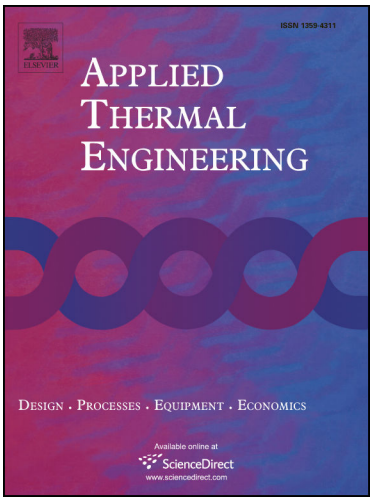

Research Paper

Feasibility analysis of a thermo-hydraulic process for reverse osmosis desalination : experimental approach

C. Lacroix, B. Guillaume, M. Perier-Muzet, D. Stitou

PII: S1359-4311(22)00657-3
DOI: https://doi.org/10.1016/j.applthermaleng.2022.118713
Reference: ATE 118713

To appear in: *Applied Thermal Engineering*

Received Date: 21 January 2022
Revised Date: 10 April 2022
Accepted Date: 19 May 2022

Please cite this article as: C. Lacroix, B. Guillaume, M. Perier-Muzet, D. Stitou, Feasibility analysis of a thermo-hydraulic process for reverse osmosis desalination : experimental approach, *Applied Thermal Engineering* (2022), doi: https://doi.org/10.1016/j.applthermaleng.2022.118713

Feasibility analysis of a thermo-hydraulic process for reverse osmosis desalination : experimental approach

C. Lacroix[a,b,c], B. Guillaume[a] , M. Perier-Muzet[a,b], D. Stitou[a]

[a] *PROMES Laboratory, UPR CNRS 8521, 66100 Perpignan, France*

[b] *University of Perpignan Via-Domitia, 66100 Perpignan, France*

[c] *GEPEA, UMR CNRS 6144, IMT Atlantique, CS 20722, 44307 Nantes, France*

Keywords: desalination, reverse osmosis, thermo-hydraulic process, renewable energy

Abstract

Reverse osmosis is a widely used desalination technique, mainly because of its low specific energy consumption. Autonomous reverse osmosis processes are increasingly developed because of their energy efficiency and the decentralization of numerous water stress areas. In this context, a reverse osmosis process powered by an innovative thermo-hydraulic desalination system using heat has been developed. This new process aims to autonomously produce fresh water from a brackish water source, compatible with the needs of a small remote village. This new reverse osmosis desalination process exploits a low temperature heat source (60-80°C) such as the one delivered by solar flat-plate collectors. The heat is then converted into hydraulic energy by a thermodynamic engine cycle in which the expansion of the working fluid directly pressurizes the brackish water by means of hydro-pneumatic tanks, while energy from high pressure brine is recovered by an innovative hydraulic cylinder. Since previous numerical work on this process shown a specific energy consumption about 12 $kWh.m^{-3}$ for a 4 $g.l^{-1}$ brackish water, which is close to performances of relatable processes, an experimental full scale prototype has been built. The work presented here shows the results of the experiments conducted on this prototype, its behavior and performances. Numerical and experimental results are compared and discussed, and confirm the feasibility of the process. These tests show a promising cyclic functioning as the numerical results suggested. The freshwater production and salinity is remaining under the drinkability limit and the experimental specific energy consumption has been calculated to 25 $kWh.m^{-3}$. In order to reach better performances, transfer tanks needs to be improved to avoid heat transfer between working fluid and saltwater which leads to condensation issues, and another hydraulic cylinder design needs to be consider to avoid gasket abrasion.

1. Introduction

More and more areas in the world are concerned by a constantly increasing water demand. Numerous desalination systems are designed and evaluated to fulfill this demand. Reverse Osmosis (RO) is the most selective membrane process and is widely used for its low energy consumption and cost (Figure 1) with almost 50% of the world desalination capacity [1]. In the context of climate change, desalination technologies are more and more powered by renewable energy sources. Solar driven desalination processes particularly fits with decentralized water production, since many areas which suffer from water scarcity also benefits of high solar irradiation [2]. RO systems designed for remote area are usually powered by photovoltaic panels (PV-RO) coupled with high pressure pumps [3]. Running a RO membrane with photovoltaic panels is an interesting solution for its high operating conditions range, but

the necessity of electrical storage rises the cost [4] and the environmental footprint of these processes [5].

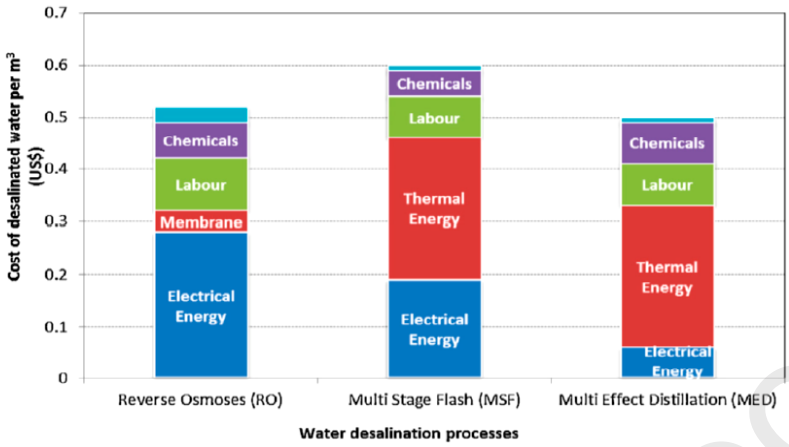

Figure 1 : Costs repartition in several desalination modes [6]

Several Solar Thermal powered RO (STRO) desalination processes are emerging through the scientific literature and gaining in maturity over the years, as Manolakos et al. [7] present it as a cheaper solution than battery-less PV-RO systems [8], [9]. Organic Rankine Cycle (ORC) is indeed a promising technique to power RO from a heat source since it includes basic and robust components [10]–[12] which enhance a lower investment cost. However, such coupled processes imply many energy conversions, leading to a drop of efficiency and exergy destruction.

A thermo-hydraulic process was designed to power reverse osmosis desalination with low-grade heat such as solar energy or waste heat, as ORC systems do. This process aims to avoid mechanical and electrical losses by directly converting thermal energy into hydraulic work and then pressurize the feed water to be desalinated. Although some theoretical studies already showed the feasibility of this kind of process using a concentrated solar source [13], [14], there is only one experimental study to the author knowledge which is evaluating such a low-grade heat source process [15]. There is then still lot of uncertainties about the coupling of a highly cycling pressurization process to a RO desalination membrane since RO systems are currently running under stable pressure constraints. Challenges of these studies are also the optimization of thermal to mechanical energy conversion. Energy transmission from the working fluid to saltwater is also challenging since it suffers from important losses and demands an effective impermeability to ensure the water drinkability.

The overall goal is to study the feasibility of a solar thermal panel powering a cyclic pressurization process coupled to a RO membrane. The main challenge is to design the components permitting thermal to mechanical energy conversion and energy recovering, chosen respectively as transfer tanks and recovery cylinder and designed especially for the process. Another challenge concerns the energy conversion that implies a highly cyclic process which makes the RO membrane resistance facing high pressure peaks up to 10 bars in few seconds. Such pressure constraints are yet few studied in the scientific literature [16], [17]. To tackle this challenges, the authors developed in a previous study the process static modelling, sizing and dynamic modelling in order to build a pilot and assess its performances [18]. Simulations results realized over a daytime showed that inertia of such thermal process would allow a stable water production, i.e. the desalination occurs even in case of cloud disturbances thanks to the solar collectors thermal mass. A next step to complete the numerical study and to established proof of concept is to build an experimental prototype.

The current study presents the design and operation of an experimental pilot of this kind of STRO process. First, the system configuration and composition are described and its functioning is explained. Then, the previous sizing and dynamic modeling is summarized with its main numerical results (see details in [18]). Data from the experimental process operation are finally presented and discussed for several running modes and set of operating conditions, and compared with numerical results.

2. Description of the system

As the thermo-hydraulic device works with a low-grade heat source (between 60°C and 100°C), this process could be run in many remote areas which benefit from a satisfying solar irradiation or even a waste heat source. Then, the heat source can be supplied by a flat plat solar collector which is a cheap and robust solution as it needs no specific material and has a lifespan of over 25 years.

The system main parts are a thermo-hydraulic engine cycle, a RO desalination unit and an energy recovery device described in Fig. 2. The engine cycle is composed by an evaporator and a condenser in which a working fluid circulates thanks to hydraulic cylinders. The working fluid out of the evaporator alternatively feeds the transfer tank, enhancing the pressurization of saltwater and pumping it into the RO membrane. The process has a cyclic working divided in two half-cycles of two phases. The first phase is a pressurization phase, the high pressure (P_h) vapour out of the evaporator goes to high pressure transfer tank to pressurize feed water. Hence, high pressure feed water passes through RO membrane to be desalinated, and the high pressure brine activates the recovery cylinder by entering the high pressure chamber. The cylinder movement triggers the pumping of feed water in one hand and the filling of the second tank in another hand. In the second phase, valve between evaporator and transfer tanks is closed, there is no more heat supplied to the working fluid. Then, the vapour in the high pressure tank expands until it fills the volume. In an ideal case, the working fluid pressure would follow an isentropic expansion. Since the pressurized water out of the tank is still higher than its osmotic pressure (P_{exp}), desalination through the RO membrane still occurs. Then, the high pressure brine finishes to push the cylinder piston until its end stroke. When this later action is over and the tank is full of working fluid, it is connected with the condenser and the first half cycle is over. Sets of valves or a distributor allow to switch transfer tanks and cylinder chambers roles, and triggered the second half cycle to begin. In each phase, the low pressure or condensation pressure (P_l) vapour coming out of the second transfer tank is transferred into the condenser to be liquefied. Independently of these phases, a pumping device (e.g. another recovery cylinder driven by the evaporator) allows the working fluid circulation between the condenser and the evaporator. The goal of this expansion phase is to improve the process performances by exploiting the most of the mechanical energy contained in the working fluid. Desalinating during the fluid expansion permits to reduce the heat needed during the pressurization, since the process is still working after this phase and without any heat source.

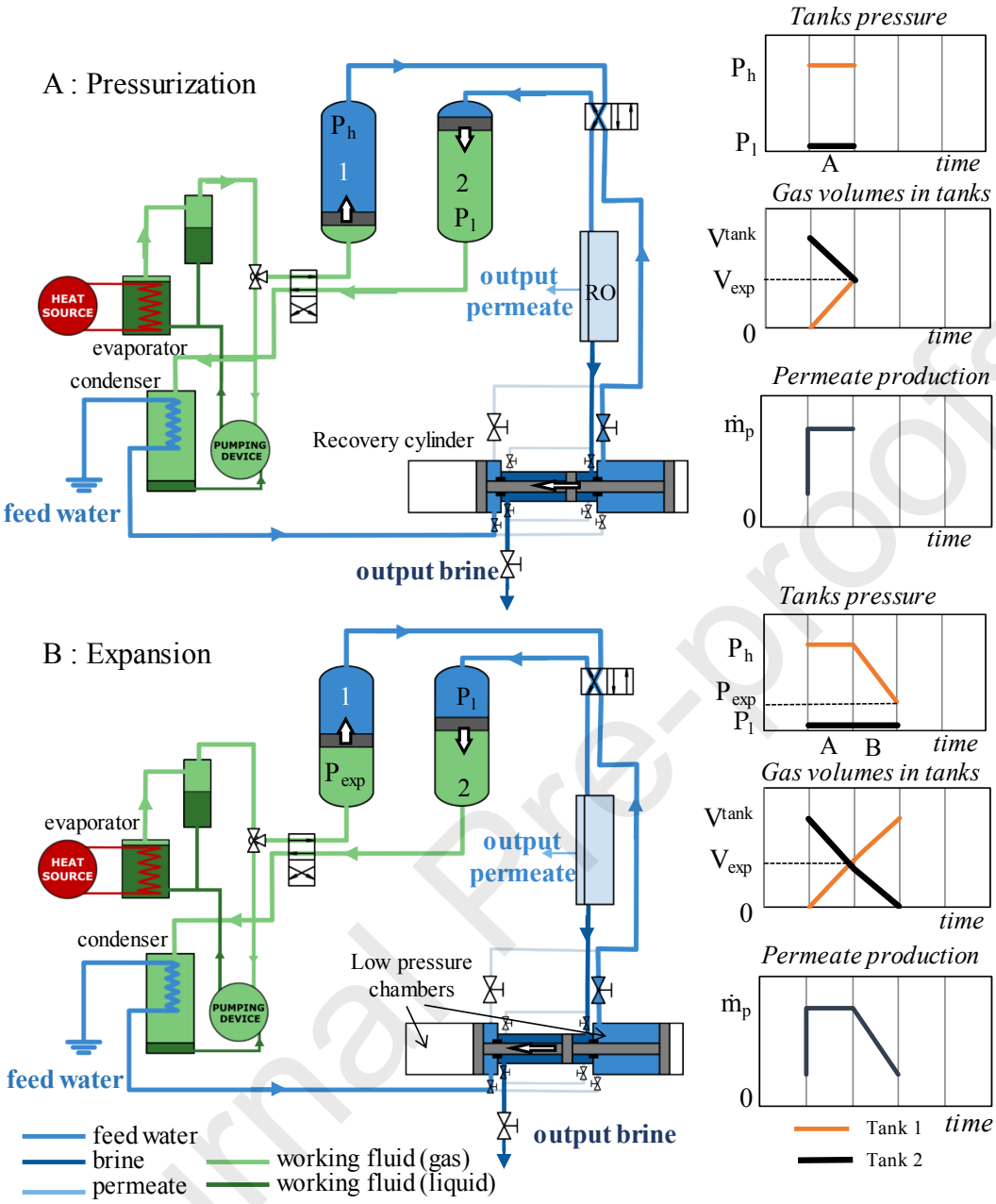

Figure 2 : Description of the two phases of process running

3. Theoretical approach

In a previous study, the authors developed both a static and a dynamic modelling approaches to respectively size the experimental prototype and study the feasibility of the overall process. The present section details the prototype sizing as well as the numerical results obtained with inputs parameters selected relatively to experimental conditions.

3.1. Prototype sizing

The previously introduced modeling study was used to design and guide the prototype conception. Sulfur Dioxide (SO_2) has been chosen as a working fluid from the preliminary study, with evaporation and condensation temperatures as selection criterion (Fig. 3). Isobutane would allow better cycle

efficiency thanks to a lower condensation temperature, but it comes with more technical constraints because of explosion risks.

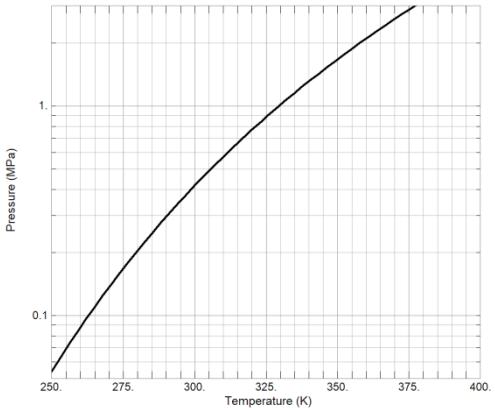

Figure 3 : Saturation curve of sulfur dioxide

A static numerical tool was firstly developed on EES Software to determine the size of main components as RO module, recovery cylinder and heat exchangers. Components were chosen to maximize the specific daily fresh water production (DWP) calculated with eq. *1* as highlighted in Fig. 4. Recovery cylinder was designed from the sizing of pistons diameter.

$$DWP = \frac{\int_{day} \dot{m}_p}{A_{sol}} \quad (1)$$

As it can be seen, the piston diameter and the membrane permeability which would allow the process to work under the largest expansion end pressure scale and with the maximum water production are respectively 100 mm and 46 liters.h^{-1}.bar^{-1}. Evaporator and condenser exchange area has been also determined about respectively 2.4 m² and 1.4 m² from these calculations to allow a correct cycling behavior. An exchanger efficacy about 0.7 was assumed for the prototype sizing.

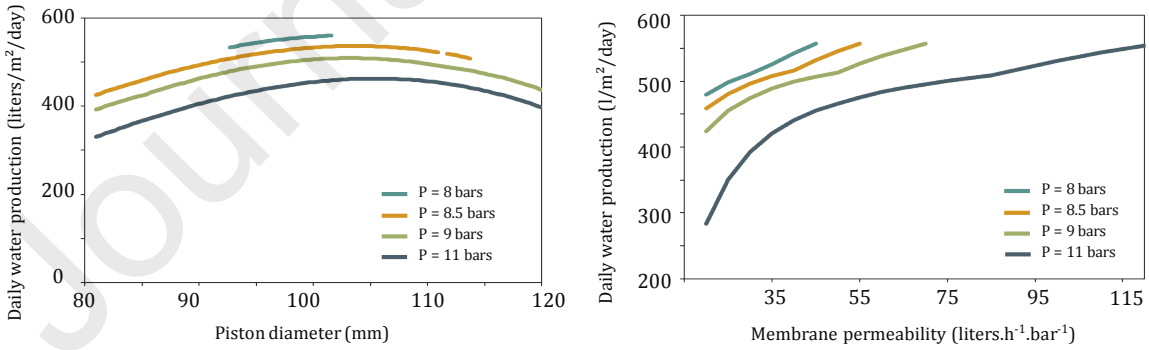

Figure 4 : Component size determination to maximize daily water production in the highest expansion pressure scale

3.2. Simulation results

Dynamic simulations have been realized using Python programming language and explicit time discretization method [18]. Simulations were run over several cycles to assess the short-term process behavior under constant input power. Numerical results show a regular cyclic running, transfer tank pressures are alternatively at equilibrium with evaporator and condenser pressures (Fig. 4a). The input

power for the presented simulation has been set to 800 W, which allows to reach an upper pressure about 14 bars in the evaporator. It can be seen in Fig. 4b that permeate flow follows the pressure profile of the membrane connected transfer tank, with a slight decrease during the pressurization phase.

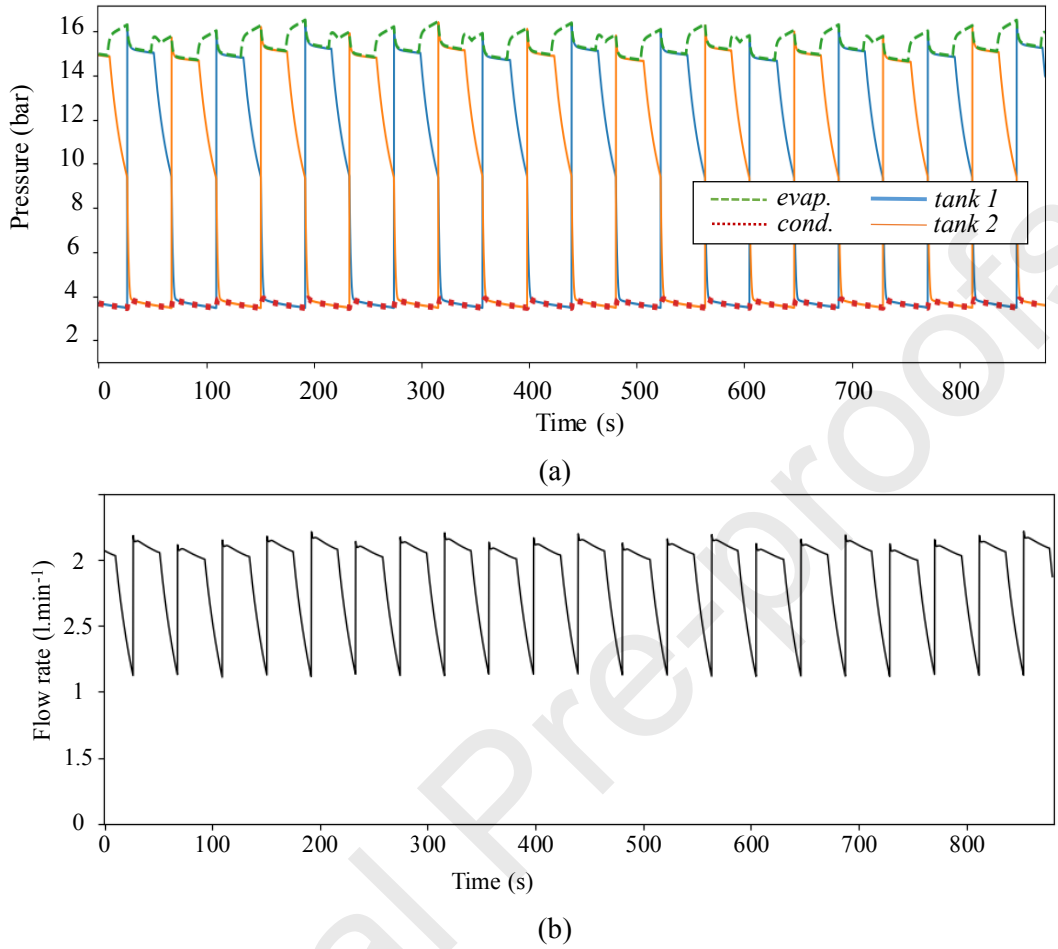

Figure 5 : Evolutions of system main outputs. (a) : Pressures in main component. (b) : Permeate flow rate

The thermodynamic cycle aims to produce work from a heat source, its efficiency η_{cycle} is therefore defined in eq. *(2* as the ratio between produced work W and supplied heat Q_{in}.

$$\eta_{cycle} = \frac{W}{Q_{in}} \tag{2}$$

The chosen thermodynamic performance indicator is the specific energy consumption (SEC) expressed in eq. *(3*. It gives the amount of required thermal energy to produce a unity of freshwater. This indicator is widely used since it gives the energy efficiency independently from the installation size.

$$SEC = \frac{Q_{in}}{\int_{day} \dot{m}_p} \tag{3}$$

This preliminary study shows that this process could offer a daily production of 500 liters per m² of solar collector area, with a SEC about 12 $kWh_{th}.m^{-3}$. These results established a first theoretical proof of feasibility of such a cyclic process as its performances are relatable to PV-RO systems which presents SEC about 10 to 30 $kWh_{eqth}.m^{-3}$ [16], [19]–[21]. Equivalent thermal energy was calculated here considering a PV panel efficiency of 15%, thus representing the incoming solar energy needed to produce a cubic meter of water.

4. Experimental set-up

Experiments were conducted on a prototype at full scale to study and evaluate the process behavior. The pilot was designed and implanted at the PROMES CNRS Laboratory (Perpignan, France). A picture of the installation is shown in Figure 6. and its corresponding flows diagram in Figure 7. The system main components are pressure accumulators, an evaporator and a condenser, a RO membrane and a hydraulic cylinder. Prototype was built without solar panel as the work focuses on the thermo-hydraulic process and no innovation is proposed about the heating technology. Temperature controlled water flow circulates in the evaporator and the condenser to ensure heating and cooling. A list of the system components and their characteristics is given in Table 1. The pipes and tanks are made out of stainless steel for the working fluid loop and PVC for the water flows.

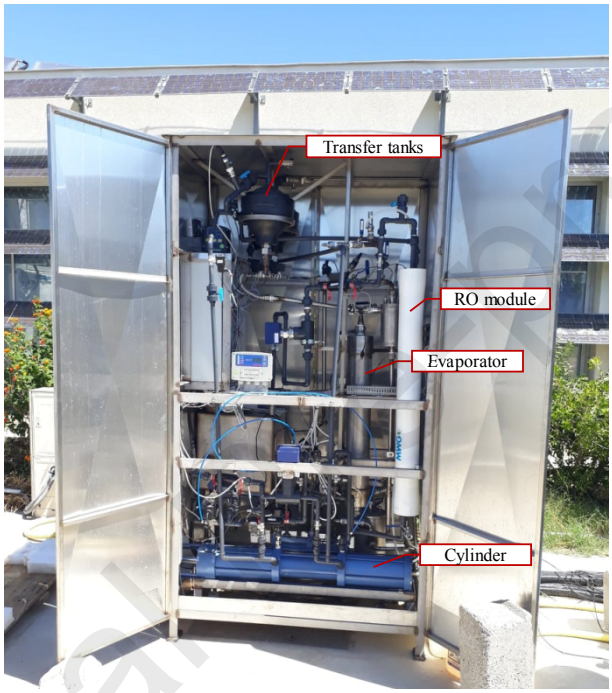

Figure 6 : Picture of prototype set-up

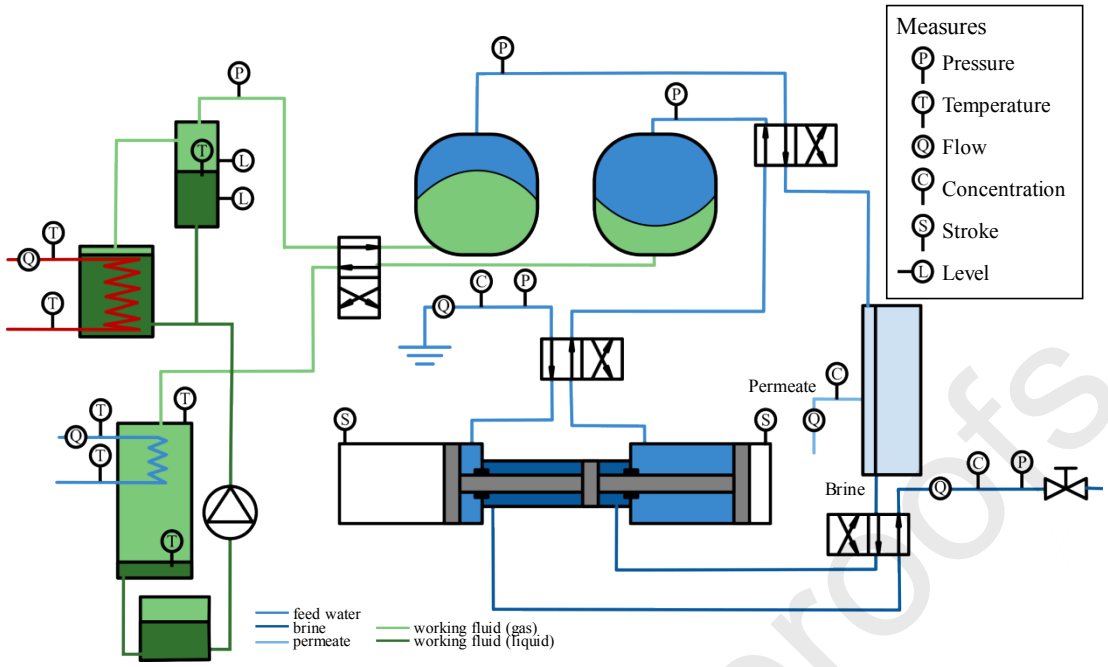

Figure 7 : Fluid and instrumentation diagram

Phase switch is operated by sets of four solenoid valves controlled by an acquisition program developed with NI LABVIEW. An electrical pump permits the working fluid transfer between condenser and evaporator. Unlike the theoretical process, condenser is not cooled by feed water entering the system. The cooling is obtained by a temperature controlled cold water loop. There is also a hot water loop which supplies heat to the evaporator. The power of the hot water loop is regulated to set the maximum reached pressure in the evaporator. The pressure accumulators are two tanks of each 3 liters. Two chambers are separated by an elastic EPDM membrane, each chamber volume can variate from 0.25 to 2.85 liters following the membrane position and can stand maximum pressure of 400 bars.

The measured outputs on the system are water conductivity, flow rate, pressure and water temperature. Main sensors are listed in Table 2 with their range and accuracy.

Table 1 : Description of process components

Component	**Design**	**Reference**
Evaporator	exchange surface of 2.4 m²	Spirec E.24.72.T
Condenser	exchange surface of 1.4 m²	Spirec EC.14.48.T
Separator	1.57 liters	Designed by ETE
Condensate tank	5 liters	Designed by ETE
Pressure accumulator	EPDM membrane, steel wall, volume of 2.85 liters	Hydroleduc AS04.P.E/4
Hydraulic cylinder	4 chambers: 2 of 3 L and 140 mm of diameter, 2 of 1.5 L and 100 mm of diameter, rod diameter of 20mm	Specialy designed by Maac Hydraulic
SO_2 Pump	30 L/h, pump to 20 bars	OBL XRN6.30
RO membrane	8.7 m² of active area, salt rejection > 99.5%	Filmtech LC.HR4040
Proportional valve	Kvs=0.12 m3/h, inox 316L	Burkert Valve 2875
Solenoid valve	Kvs= 0.24 m3/h or 0.21 m3/h (reverse flow)	ODE 21L2K1T30

Table 2 : Characteristics of sensors

Sensor	Range	Accuracy	Reference
Conductivity meters	0-1 mS/cm	1.5% of the range	Jumo CTI 750
	0-50 mS/cm	1% of the range	
Thermal loops flowmeter	1-15 L/min	0.5% of the range	Gems Sensors FT-110
Stroke sensor	0-200 mm	0.055 mm	Balluff BTL120H
Flowmeter	0.02-5 L/min	1.1% of the reading for linearity	Titan Atrato 740
Pressure sensor	0-25 bar gauge	0.5% of the range	Endress Hauser PMP11

During the tests, several input parameters were controlled to assess the process behavior. Flow rate and temperature of hot and cold water sources feeding respectively evaporator and condenser were regulated while ambient temperature was ranging between 15°C and 20°C over the experiments period.

5. Results and discussions

Experimental study has been carried out with two cycling conditions. In the first one, tests have been realized without expansion phase, whereas the working fluid was expanding at the end of the pressurization phase during the second set of tests. Results of these two kind of tests are described and discussed in this section.

5.1. Tests without expansion phase

A first set of tests was carried out maintaining a constant pressure in the transfer tanks, i.e. without expansion phase. The system was operated on a time period about 1 hour, which represents around 11 cycles. In this time-lapse, no disturbances were observed over the cycles. In that case, pressure in the feed tank is always near to evaporator high pressure. Hot water temperature in the evaporator was set to 65°C, leading to a heating power about 750 W, and the feed water salinity was around 4 g/L. Figure 8a shows the pressures evolutions in the main components. It can be seen that pressures in the transfer tanks are alternatively equivalent to the evaporator and condenser ones. It should be noticed that the pressure control is efficient since the pressure variations in the exchangers are minor.

These measures show that the pressure losses between the tanks and the exchangers are quite low, less than 0.2 bar. With these operating conditions, cycles last around 150 seconds, the lower pressure is 4 bars and upper pressure is 10 bars. Temperature of hot and cold sources are relatively stable with evaporation temperature around 55 °C with small variations about 3-4°C. Condensation temperature is more constant around 20°C. It can be seen that disturbances occur during some half-cycle changings. Fig. 8b describes the permeate flowrate evolution. Given the Darcy law, the permeate flow should follow the feed tank pressure tendency as showed by the numerical simulation in Fig. 4, but experimental results show it is not the case. The flowrate stopped whereas pressure in the tank is still higher than feedwater osmotic pressure. The drop of permeate flow following the peak can be explained by the appearing of a diffusive layer at the membrane wall. This phenomenon is named polarization and is known to cause the decrease of permeate flux in time [22]. The flow stopped suddenly when maximum brine volume needed to fill the cylinder is reached, by closing a valve. The fact that the maximum brine quantity is reached before the half-cycle end means that the RO membrane is oversized and its permeate flow is higher than the values taken in sizing and simulations. Fresh water salinity (measured here through

conductivity) is between 300 ± 5 and 150 ± 2.5 mg/liters which is lower than the freshwater drinkability limit. These first tests show that the sudden high pressure peaks do not impact membrane performances on a short time lapse.

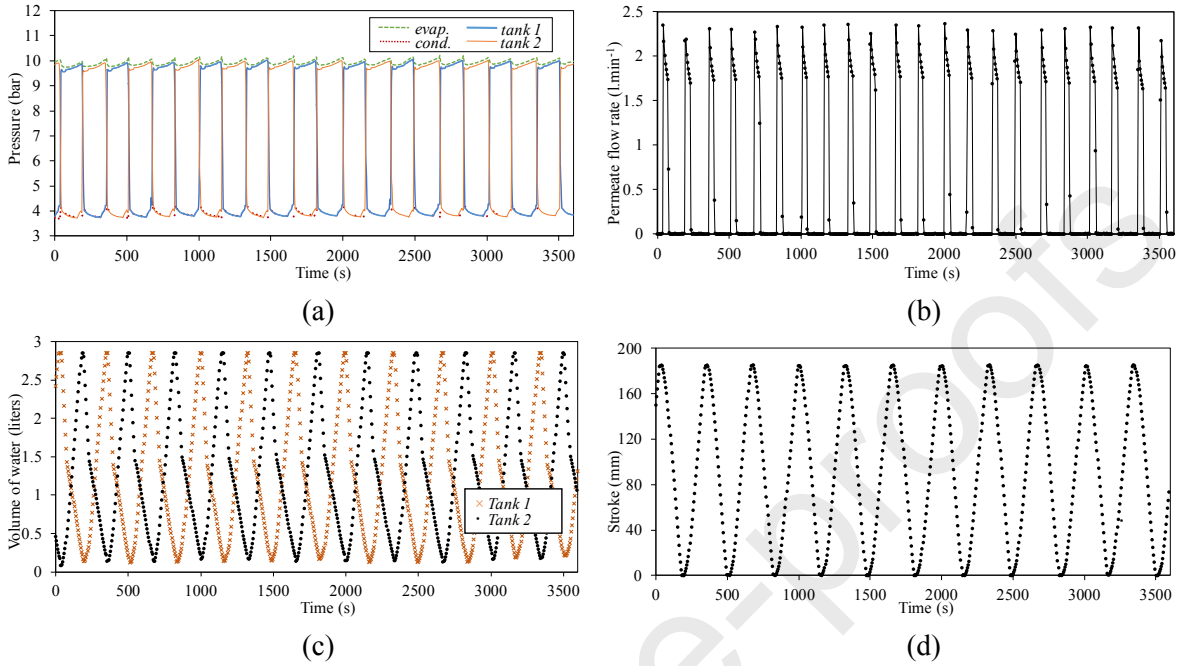

Figure 8 : Evolution of the major outputs during test without expansion phase. (a) :Pressure in main components. (b) : Permeate flow rate. (c) : Water evolution in transfer tank. (d) : Piston stroke of recovery cylinder

Water level evolutions in transfer tanks are plotted in Fig. 8c. The alternation of phases is clearly observed through changes of slope in the level path. An important change of slope can be noticed during pressurization phase, while the water volume decreases, precisely when the permeate production stopped. These curves show that transfer tanks are symmetrically fully filled and empty over the cycles.

Fig. 8d shows piston position of cylinder over cycles. It appears that the piston behavior is symmetric and goes until its end stroke at each half cycle. The piston stroke evolution is linear since the motor piston is driven by controlled brine flow rate which is maintained constant.

This first set of experiments confirms that the process configuration allows a continuous working as expected in the design phase. However, this configuration is not fully optimal since at the end of each half cycle, all of high pressure working fluid is evacuated. This implies a major loss of the mechanical work. To exploit this additional work, another operating is tested in which the half cycles are divided in two phases, a phase of pressurization and a phase of expansion until the feed water osmotic pressure is reached in the feed tank.

5.2. Tests with complete cycle

The second set of tests was then conducted including the expansion phase of each half cycle. The feed water salinity remains 4 $g.l^{-1}$, the power is about 1.5 kW. Transition between pressurization and expansion phase is calculated with perfect gas law fixing a pressure at the end of the expansion, i.e. the tank is full of gas. Figure 9 shows the pressures evolution in transfer tanks and in exchangers.

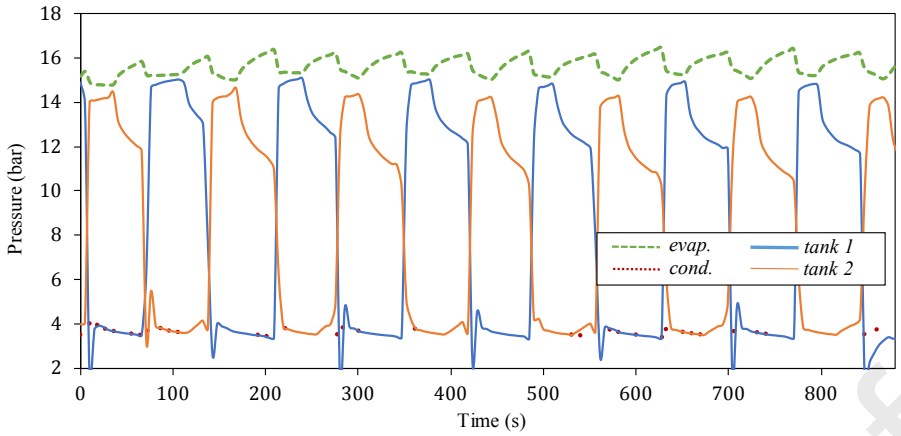

Figure 9 : Pressure evolution in main components during test with expansion phase

By plotting water level evolution in the transfer tanks, it appears that one of them is not behaving as expected. Indeed, it can be observed that the later has an important dead space about the half of its volume. The explanation is a feedwater leak appearing in one of the low pressure recovery cylinder chambers. When the recovery cylinder is filling one the transfer tanks with feedwater, a small part escapes by the gasket piston. In consequence, less feedwater has been transferred to the tank as it has the same volume than the cylinder low pressure chamber. This is the reason why there is a tank which always contains an important dead space of gas which repeat over the cycles. It should be noticed same level of pressure than simulations (Fig. 5) have been obtained with an inlet power of two times higher, it shows that the energy losses related hypothesis were underestimated.

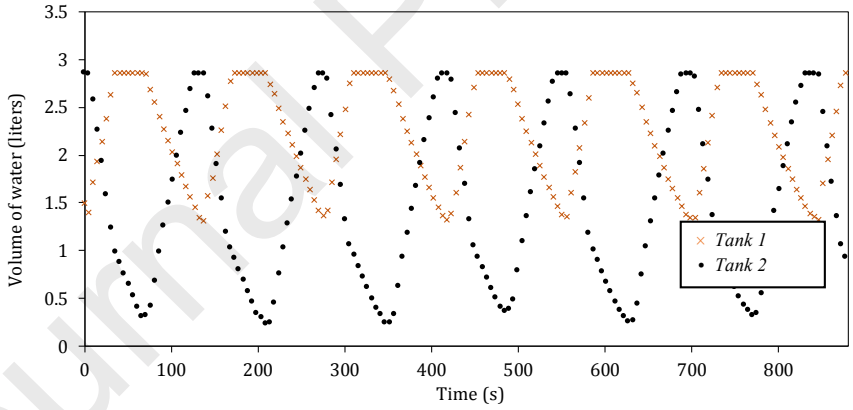

Figure 10 : Volume of water evolution in transfer tanks

The leak in the recovery cylinder has a direct impact of the permeate flow (Figure 11). On the half cycle corresponding to the transfer tank misfiling, the permeate flow is much lower, producing 80% less freshwater quantity over the half cycle. It can be explained by the limited quantity of feedwater contained in the tank, since this quantity has a direct impact on the permeate quantity produced over the half cycle. However, in the normally working half cycle, the amount of produced freshwater corresponds to the numerical results. It shows that the link between permeate production and transfer tank pressure was modelled with correct hypothesis. Moreover, these results confirm that the RO membrane seems not impacted by high pressurization peaks over the experimentation time as no permeate production decrease has been recorded on the working half cycle.

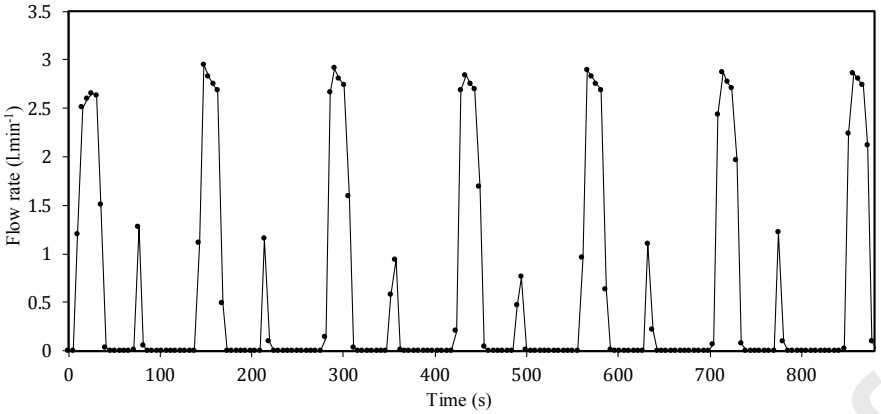

Figure 11 : Evolution of conductivity and flow rate of produced freshwater

Figure 12 describes the engine cycle on a P-V diagram from which is computed the mechanical work over the cycles. The cycle efficiency is therefore calculated using eq. *(2*, and represents the ratio between work supplied to feed water and inlet heat. These results show that the cycle efficiency can reach 7% which is relatable to ORC efficiencies [23]. Phases can be distinguished in the graph regarding the pressure evolution. Phases at constant high and low pressures corresponds respectively to tanks gas filling and exhaust. The part where the pressure is variating with the volume corresponds to the expansion phase.

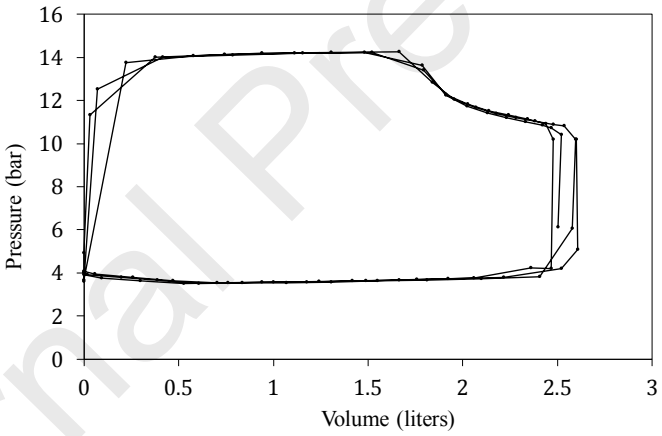

Figure 12 : P-V diagram of working fluid in a transfer tank

5.3. Evaluation of water salinity influence

Another salinity range was tested to evaluate its influence on the process behavior. The selected other value of water salinity was 6 g/l, which is 50% more than feedwater salinity of previous tests. The process behavior was studied for two values of the heating power, i.e. with two heating transfer fluid temperature of 65°C and 80°C. It leads to two tested powers of respectively 1 kW and 2 kW. These results presented in Figure 13 demonstrates that the process can be run for higher salinity, as the membrane design aims to.

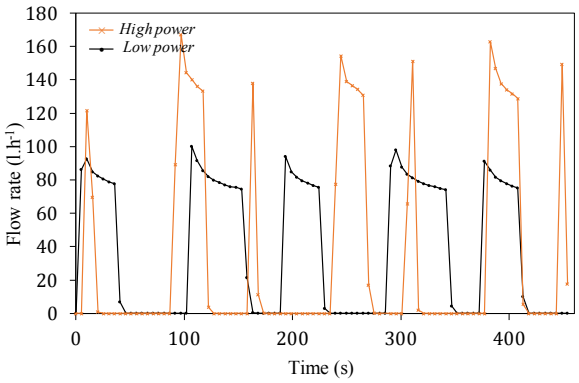

Figure 13 : Permeate flow rate comparison for two heating powers with feedwater concentration of 6 g/l

The trends are similar compared to the previous set of tests done with a feed water salinity of 4 $g.l^{-1}$. With higher input power, cycles are quicker but pressure losses during the pressurization phase are higher as well. Despite the absence of the expansion phase, the test at high pressure shows the same asymmetry observed in the test with expansion phase. Both of these flawed tests have been realized at higher pressure, leading to an increase of the leak in the cylinder which restrains the complete filling of one of the transfer tanks.

5.4. Discussions about the results

Several conclusions and interpretations can be made regarding these experimental results. From the operating conditions tested, it appears that the system works well with only pressurization phases. The permeate production is high because the pressure is always high, but it implies an important energy consumption since a part of the mechanical work is not used. Thus, adding an expansion phase in the half cycle as it is presented previously seems to allow a more energy efficient running.

Results from these tests are promising but shows for this later set of tests that some disturbances occur over the cycle due to conception flaws. Cylinder piston gaskets have been deteriorated through the cycles, leading to a leak in one of the chambers. Consequences are inefficient filling of one of the transfer tanks, leading to severe drop of permeate production in the half cycle. This leak made the comparison with numerical results on one of the half cycles difficult and has impacts on the overall performances of the process. This defect is not easily correctible in the prototype since the recovery piston has been tailor-made for the study, and its origin seems to be a fooling problem. A first solution could be to oversize the low pressure chamber to overcome this issue. Since, energy losses come essentially from evaporator, separator and condensation in the transfer tanks, it is thus necessary to improve the insulation of these components. Evaporator heat losses have been quantified about 150 W to 220 W (for input heat power about 750 W to 1.5 kW) which represents 15-20% of losses and then an important source of performance degradation. Condensation appearing in transfer tanks is due to heat transfer across the membrane separating saltwater from working fluid, but it could not be quantified because adding sensors in the tanks was possibly destructive. As there is always cold water in the transfer tanks, the membrane temperature remains cold and leads to working fluid condensation. Analytical extrapolations have been computed on the process performance in the absence of the recovery cylinder leak. Calculations show that the system can reach a SEC about 25 $kWh.m^{-3}$ following the previous tests conditions, which is not including the electrical consumption. This energy consumption appears to be twice as the numerical one, which is not surprising given the high amount of energy lost in the non-insulated evaporator and the condensation occurring in the transfer tanks.

These losses can be avoided by minimizing the heat transfer between saltwater and working fluid inside the transfer tanks, but no relevant membrane technology has been found yet. A solution could be another

technology as the one studied by Godart [24], i.e. separating working fluid from saltwater in two distinct chambers and assuming the motion transfer by two connected pistons. This system implies more friction and mechanical losses, but ensure there is not contact between water and working fluid, which is a solution to condensation issues and sanitary constraints.

From these tests it appears that the process is mostly running as expected. Pressures losses between evaporator and transfer tanks are low, leading to an efficient pressurization phase. However, permeate production is not following the transfer tank high pressure. Given the Darcy's law, it means that there are pressure losses between transfer tanks and the RO membrane, which is confirmed by the delay observed between the membrane permeation and the tank pressurization.

Moreover, these results show that the cycling is working well and cycles quality is not worsening over the time. It means the process as it has been designed permits to realize a cyclic working at real scale with acceptable freshwater production and quality with a hot source around 60°C and a cold source around 20°C. These conditions are suitable to a coupling with a large range of low-grade solar or waste heat sources, whereas 20°C is a cold source temperature easily reachable. The novel cylinder technology for water pumping and circulation is very promising since the gasket damaging problem seems the major remaining technical issue.

6. Conclusion

This paper presented experiments on a thermo-hydraulic desalination process. For the purpose of this study, a scale up prototype was built, instrumented and run. This work follows a numerical analysis and complete the overall feasibility study of the desalination process. For the current study, new hydraulic components were designed, such as the transfer tanks and the recovery cylinder. This novel approach led to some challenges in process operation and results interpretation. Indeed, several leaks and permeability issues appeared and impacted consequently the process behavior and the overall performances.

This experimental study shows that the overall designed process allows a controlled functioning by managing the tests conditions such as hot and cold temperature or flows, and it mostly behaves as the numerical study predicted.

It can be seen from the two different tests that adding an expansion impacts the process. Expansion phase rises the cycle efficiency but implies difficulties in the process setup as it needs more inlet power to work. The results showed that the kind of dynamic inducted by the process behavior has minor impacts on the RO membrane behavior as there is no noticeable desalination performance decrease over the cycle accumulation. Extrapolations of performances were calculated for the test with expansion phase and highlights interesting SEC when considering processes of the same kind.

These works proved the feasibility of a coupling between thermo-hydraulic process and RO desalination powered by low-grade heat source. Such process which can be run with a 60°C heat source and an ambient temperature cold source allows a wide range of couplings and applications by its modularity and its resilience. The thermodynamic cycle as it is designed fulfill its role of water pressurization, and it has been shown that dynamics of working cycles does not impact the RO membrane behavior, even in the long run. Thus, some improvements have to be done to get the process mechanized. The conception of recovery cylinder has to be revised to avoid gasket degradation in time. A new membrane material or a new technology also has to be found to ensure a hermetic and insulating separation of water and working fluid, which is a major health concern. The resolution of the technical issues could allow to quantitatively compare and validate experimental and experimental and numerical results. Afterward,

an autonomous demonstration pilot would be designed to perform the techno-economic assessment that are needed before a potential scaling up to industrialization.

Acknowledgments

The authors wish to acknowledge the SATT AxLR and LabEx SOLSTICE laboratory for their financial support on this project. This work was supported by the French Program "Investissements d'Avenir" (Investment for the Future) of the French National Agency for Research (ANR) under award number ANR-10-LABX-22-01-SOLSTICE. The authors also thank Mr. D. Ginestet, J. Benard, J.J. Huc and E. Hernandez for their technical assistance on the experimentations, and J. Hemmer for her advice on paper structure.

List of symbols

m : mass
$\dot{m}$: mass flow
P : pressure
Q : heat energy
$\dot{Q}$: heat power
V : volume
Y: RO membrane conversion rate
$\dot{W}$: mechanical power
η : efficiency

Subscripts

cycle : thermodynamic cycle
exp : expansion
f : feedwater
h : high
in : inlet
l : low
p : permeate
tank : transfer tank

References

[1] M. Qasim, M. Badrelzaman, N. N. Darwish, et N. A. Darwish, « Reverse osmosis desalination : A state-of-the-art review », vol. 459, nº December 2018, p. 59‑104, 2019, doi: 10.1016/j.desal.2019.02.008.

[2] A. Pugsley, « Global applicability of solar desalination », *Renew. Energy*, vol. 88, p. 200‑2019, 2016.

[3] F. E. Ahmed, R. Hashaikeh, et N. Hilal, « Solar powered desalination – Technology, energy and future outlook », *Desalination*, vol. 453, p. 54‑76, mars 2019, doi: 10.1016/j.desal.2018.12.002.

[4] E. Sh. Mohamed, G. Papadakis, E. Mathioulakis, et V. Belessiotis, « A direct coupled photovoltaic seawater reverse osmosis desalination system toward battery based systems — a technical and economical experimental comparative study », *Desalination*, vol. 221, nº 1‑3, p. 17‑22, mars 2008, doi: 10.1016/j.desal.2007.01.065.

[5] A. C. Schomberg, S. Bringezu, et M. Flörke, « Extended life cycle assessment reveals the spatially-explicit water scarcity footprint of a lithium-ion battery storage », *Commun. Earth Environ.*, vol. 2, nº 1, p. 11, déc. 2021, doi: 10.1038/s43247-020-00080-9.

[6] I. Ullah et M. Rasul, « Recent Developments in Solar Thermal Desalination Technologies: A Review », *Energies*, vol. 12, nº 1, p. 119, déc. 2018, doi: 10.3390/en12010119.

[7] D. Manolakos, E. Sh. Mohamed, I. Karagiannis, et G. Papadakis, « Technical and economic comparison between PV-RO system and RO-Solar Rankine system. Case study: Thirasia island », *Desalination*, vol. 221, nº 1‑3, p. 37‑46, mars 2008, doi: 10.1016/j.desal.2007.01.066.

[8] M. Thomson et D. Infield, « A photovoltaic-powered seawater reverse-osmosis system without batteries », vol. 153, p. 1‑8, 2002.

[9] A. Soric, R. Cesaro, P. Perez, E. Guiol, et P. Moulin, « Eausmose Project–desalination by Reverse Osmosis and Batteryless Solar Energy: Design for a 1m3 Per Day Delivery », *Procedia Eng.*, vol. 44, p. 1465‑1467, 2012, doi: 10.1016/j.proeng.2012.08.830.

[10] C. Li, S. Besarati, Y. Goswami, E. Stefanakos, et H. Chen, « Reverse osmosis desalination driven by low temperature supercritical organic rankine cycle », *Appl. Energy*, vol. 102, p. 1071‑1080, févr. 2013, doi: 10.1016/j.apenergy.2012.06.028.

[11] D. Manolakos, G. Papadakis, E. S. Mohamed, S. Kyritsis, et K. Bouzianas, « Design of an autonomous low-temperature solar Rankine cycle system for reverse osmosis desalination », *Desalination*, vol. 183, p. 73‑80, 2005.

[12] B. F. Tchanche, G. Lambrinos, A. Frangoudakis, et G. Papadakis, « Exergy analysis of micro-organic Rankine power cycles for a small scale solar driven reverse osmosis desalination system », *Appl. Energy*, p. 12, 2010.

[13] P. Godart, « Design and simulation of a heat-driven direct reverse osmosis device for seawater desalination powered by solar thermal energy », *Appl. Energy*, vol. 284, p. 116039, févr. 2021, doi: 10.1016/j.apenergy.2020.116039.

[14] A. A. A. Attia, « Thermal analysis for system uses solar energy as a pressure source for reverse osmosis (RO) water desalination », *Sol. Energy*, p. 8, 2012.

[15] O. N. Igobo, « Isothermal Organic Rankine Cycle (ORC) driving Reverse Osmosis (RO) desalination_ Experimental investigation and case study using R245fa working fluid », *Appl. Therm. Eng.*, p. 7, 2018.

[16] B. S. Richards, D. P. S. Capão, W. G. Früh, et A. I. Schäfer, « Renewable energy powered membrane technology: Impact of solar irradiance fluctuations on performance of a brackish water reverse osmosis system », *Sep. Purif. Technol.*, vol. 156, p. 379‑390, déc. 2015, doi: 10.1016/j.seppur.2015.10.025.

[17] D. Cheddie, « Transient modeling of wave powered reverse osmosis », *Desalination*, vol. 260, p. 153‑160, 2010.

[18] C. Lacroix, M. Perier-Muzet, et D. Stitou, « Dynamic Modeling and Preliminary Performance Analysis of a New Solar Thermal Reverse Osmosis Desalination Process », *Energies*, vol. 12, nº 4015, 2019.

[19] G. E. Ahmad et J. Schmid, « Feasibility study of brackish water desalination in the Egyptian deserts and rural regions using PV systems », *Energy Convers. Manag.*, p. 9, 2002.

[20] Singfoong Cheah, « Photovoltaic Reverse Osmosis Desalination System », 2004, doi: 10.13140/RG.2.1.1559.4724.

[21] M. A. Alghoul, « Design and experimental performance of brackish water reverse osmosis desalination unit powered by 2 kW photovoltaic system », *Renew. Energy*, p. 14, 2016.

[22] S. Sablani, M. Goosen, R. Al-Belushi, et M. Wilf, « Concentration polarization in ultrafiltration and reverse osmosis: a critical review », *Desalination*, vol. 141, nº 3, p. 269‑289, déc. 2001, doi: 10.1016/S0011-9164(01)85005-0.

[23] L. Branchini, A. De Pascale, et A. Peretto, « Systematic comparison of ORC configurations by means of comprehensive performance indexes », *Appl. Therm. Eng.*, vol. 61, nº 2, p. 129-140, nov. 2013, doi: 10.1016/j.applthermaleng.2013.07.039.

[24] P. Godart, « Heat-driven direct reverse osmosis for high-performance and robust ad hoc seawater desalination », *Desalination*, vol. 500, p. 114800, mars 2021, doi: 10.1016/j.desal.2020.114800.

- A prototype of solar thermal process for reverse osmosis desalination has been built
- Low-grade solar heat can be used to run a reverse osmosis process
- Theoretical and experimental results were carried out to prove the feasibility of the process
- Experimental results from the process prototype showed a Specific Energy Consumption about 25 $kWh.m^{-3}$
- Performances can be improved by solving technical issues as leakage in the cylinder and insufficient evaporator insulation

Declaration of interests

☒ The authors declare that they have no known competing financial interests or personal relationships that could have appeared to influence the work reported in this paper.

☐ The authors declare the following financial interests/personal relationships which may be considered as potential competing interests: